



Neural correlates of spontaneous deception: A functional near-infrared spectroscopy (fNIRS) study [☆]

Xiao Pan Ding ^{a,b}, Xiaoqing Gao ^c, Genyue Fu ^{a,**}, Kang Lee ^{d,e,*}

^a Hangzhou College of Preschool Teacher Education, Zhejiang University, Hangzhou, 310012, China

^b School of Psychology and Cognitive Science, East China Normal University, Shanghai, 200062, China

^c Centre for Vision Research, York University, Toronto, ON M4N 3M6, Canada

^d Dr. Eric Jackman Institute of Child Study, University of Toronto, Toronto, ON M5R 2X2, Canada

^e Department of Psychology, University of California, San Diego, La Jolla, CA 92093-0109, USA

ARTICLE INFO

Article history:

Received 5 June 2012

Received in revised form

12 December 2012

Accepted 13 December 2012

Available online 20 January 2013

Keywords:

Deception

Neural correlates

Functional near-infrared spectroscopy

Cross correlation

ABSTRACT

Deception is commonly seen in everyday social interactions. However, most of the knowledge about the underlying neural mechanism of deception comes from studies where participants were instructed when and how to lie. To study spontaneous deception, we designed a guessing game modeled after Greene and Paxton (2009) "Proceedings of the National Academy of Sciences, 106(30), 12506–12511", in which lying is the only way to achieve the performance level needed to end the game. We recorded neural responses during the game using near-infrared spectroscopy (NIRS). We found that when compared to truth-telling, spontaneous deception, like instructed deception, engenders greater involvement of such prefrontal regions as the left superior frontal gyrus. We also found that the correct-truth trials produced greater neural activities in the left middle frontal gyrus and right superior frontal gyrus than the incorrect-truth trials, suggesting the involvement of the reward system. Furthermore, the present study confirmed the feasibility of using NIRS to study spontaneous deception.

© 2013 Elsevier Ltd. All rights reserved.

1. Introduction

Deception is common in our everyday lives (DePaulo et al., 2003). It occurs in politics, business, diplomacy, sports, friendships, and even family relationships. Extensive behavioral research has been devoted to examining deception in adults and children (Crossman & Lewis, 2006; Fu & Lee, 2007; Talwar & Lee, 2008; Xu, Bao, Fu, Talwar, & Lee, 2010). With technological improvements in recent decades, it is now possible to use various new imaging tools to study the neural mechanisms of deception (for reviews, see Abe, 2011; Christ, Van Essen, Watson, Brubaker, & McDermott, 2009).

One of the most prevalent paradigms used in neuroimaging studies of deception is the Guilty Knowledge Test (GKT). The GKT is a test of prior knowledge of event details that would be known only to a person involved in the event. By comparing the person's different responses between deceptive and control items, one can

glean behavioral, physiological, or neural markers of deception (Gamer, Klimecki, Bauermann, Stoeter, & Vossel, 2009). Most of the functional magnetic resonance imaging (fMRI) studies using GTK have found deception-related activities in the frontal cortex, such as the prefrontal cortex (PFC) and anterior cingulate cortex (ACC), regardless of differences in task demands. For example, Langleben et al. (2002) asked participants to hide a card in their pockets and then to deny the possession of the card. They found increased activity in the superior frontal gyrus (SFG) and ACC when deceptive responses were contrasted with truthful responses.

In addition to GKT, other paradigms have been developed. Ganis, Kosslyn, Stose, Thompson, and Yurgelun-Todd (2003) asked participants to generate lies based on rehearsed and unrehearsed false information related to their past autobiographical experiences. Both types of lies elicited more activations than truth-telling in the bilateral anterior prefrontal cortices. Nuñez, Casey, Egner, Hare, and Hirsch (2005) asked participants to perform a yes/no memory test for autobiographical knowledge (e.g., 'Can you ride a bicycle?') as well as for non-autobiographical knowledge (e.g., 'Is New York City in Ohio?'). They found increased activity associated with lying relative to truth-telling in the dorsolateral prefrontal cortex (DLPFC) and ACC. Recently, Abe et al. (2008) conducted an fMRI experiment to explore the specificity of prefrontal activity in intentional deception, and confirmed that prefrontal activity was specifically associated with

[☆] Author note: The present study was supported in part by grants from the National Science Foundation of China (31070894) and Program for Innovative Research Team in Zhejiang Normal University to Genyue Fu as well as grants from SSHRC and NIH (R01 HD047290) to Kang Lee.

* Corresponding author at: Dr. Eric Jackman Institute of Child Study, University of Toronto, 45 Walmer Road, Toronto, Ontario, M5R 2X2, Canada.

** Corresponding author.

E-mail addresses: fugy@zjnu.cn (G. Fu), kang.lee@utoronto.ca (K. Lee).

the generation of deceptive responses, not simply reflecting untrue responses. The pivotal role of the PFC on deception has also been supported causally by a transcranial direct current stimulation (tDCS) study (Karim et al., 2010). Thus, despite the use of different paradigms, most of the existing studies have consistently found deception-related activity in the PFC and ACC (Abe, 2009; Christ et al., 2009; Gamer et al., 2009; Ganis, Morris, & Kosslyn, 2009; Greene & Paxton, 2009; Kozel, Padgett, & George, 2004).

The activations in these areas are not surprising because such findings are consistent with the conceptualization of deception as an executive control intensive task (Langleben, 2008; Langleben et al., 2002; Sip, Roepstorff, McGregor, & Frith, 2008; Spence et al., 2001; Vrij, Fisher, Mann, & Leal, 2006). To deceive, one must inhibit the disclosure of the true state of affairs and instead present publicly a false state of affairs. To do so requires a host of executive functions such as inhibition, working memory, and cognitive flexibility (Abe, 2009; Christ et al., 2009; Gombos, 2006; Johnson, Barnhardt, & Zhu, 2004; Talwar & Lee, 2008). The PFC and ACC have been consistently found to be involved in these executive functions (Fassbender et al., 2004; Osaka et al., 2004).

However, most of the existing studies typically instructed participants when and how to lie. Participants did not lie out of their own volition. The targets of the participants' lies were usually the experimenters themselves who were aware of their deception. One potential problem with these existing paradigms is that by asking participants to lie according to the experimenters' instructions, participants may not be as motivated to deceive as they would in real world situations (Sip et al., 2008). In the real world, individuals tell lies spontaneously: they not only form a deceptive intent on their own, but also come up with their own false statements to deceive, and decide when to deploy their deception. In addition, the target of the deception is usually unaware of the deceiver's deceptive intention.

To date, only one study has explored the neural mechanisms underlying spontaneous deception. Greene and Paxton (2009) asked participants to predict the outcomes of coin flips to gain monetary reward in an fMRI study. In one half of the trials, participants were rewarded according to self-reported correct predictions, and therefore had an opportunity to gain money by saying that their incorrect predictions were correct ones (the opportunity condition); in the other half of the trials, they did not have such an opportunity (the no opportunity condition). Participants who reported improbably high levels of accuracy in the opportunity condition ($> 69\%$; M accuracy = 84%) were classified as "dishonest", and those who reported the lowest probable accuracy rate (M accuracy = 52%) as "honest". The dishonest individuals showed increased prefrontal activity in the opportunity condition compared to the no opportunity condition, while the honest individuals did not show such a difference.

While the work by Greene and Paxton (2009) revealed significant differences in prefrontal activity between individuals who spontaneously lied and those who did not, close inspection of their findings suggest that the "dishonest" participants did not lie all the time. Given the fact that these participants' accuracies ranged from 69% to about 95% in the opportunity condition, it is likely that they sometimes lied and sometimes told the truth about their incorrect predictions. Due to the specific experimental design by Greene and Paxton, it could not be ascertained exactly in which trials the participants lied or told the truth about their incorrect predictions. Thus, it is not clear whether neural activities would differ between the trials where the dishonest individuals spontaneously lied and the trials where the same individuals spontaneously told the truth.

All the existing neural imaging studies that examined experimenter-instructed lying have compared neural activities between lies and truths told by the same participants. Examining

spontaneous lies and truths by the same individuals would allow for the comparison of neural activities during spontaneous deception with those revealed by the existing studies using instructed deception. If the two types of deception engender similar neural activities and regions, it would address a perennial criticism that the existing findings lack ecological validity due to the "unnaturalistic" procedures that have been used thus far in the field (Sip et al., 2008).

In the current study, we developed a guessing game that enabled participants to lie spontaneously in a naturalistic situation similar to the opportunity condition in Greene and Paxton (2009) study. Our procedure also allowed us to precisely classify each trial as either lying or truth-telling. During this game, participants were instructed to guess which side of the screen a coin would appear on and to make their prediction by moving their corresponding hand under a desk (the experimenter thus could not see their predictions). Following their prediction, participants reported whether they guessed correctly. Participants were told that they would receive points for guessing correctly and lose points for guessing incorrectly, and they had to obtain enough points to end the game and receive a payment. Since participants knew that the experimenter could not see their hand movements under the desk, it created an opportunity for them to lie by telling the experimenter that they were correct when they predicted incorrectly. However, unbeknownst to the participants, hidden video cameras captured their hand movements so that we could check whether the participants lied to be correct when they in fact predicted incorrectly (incorrect-lie), told the truth when they predicted incorrectly (incorrect-truth), or told the truth when they in fact guessed correctly (correct-truth).

To further ensure ecological validity, we used the near-infrared spectroscopy (NIRS) methodology to collect neural responses during this guessing game. It should be noted that the current NIRS methodology has relatively poorer spatial resolution than MRI. For example, due to its limitations, the NIRS methodology only allows for collecting cortical activation data as deep as 15–25 mm beneath the scalp. Despite this limitation, the NIRS system's portability and quietness makes it possible for the participants to interact with the target (the experimenter) in a naturalistic manner. Also, the NIRS methodology allows for the collection of both oxygenated and deoxygenated hemoglobin activity simultaneously: information gleaned from the two types of hemoglobin activity sometimes complements each other to reveal significant neural activity that may not otherwise be detected (Lloyd-Fox, Blasi, & Elwell, 2010). In addition, because our NIRS equipment has a 10 Hz sampling rate, with the use of a slow event-related design, we could obtain the actual time course of the neural activity for individual trials. Such data allow us to derive grand averaged event-related oxygenated hemoglobin ([oxy-Hb]) and deoxygenated hemoglobin ([deoxy-Hb]) signal changes for a particular event (e.g., lying or truth-telling) such that [oxy-Hb] and [deoxy-Hb] signal change peaks and latencies can be obtained.

According to previous studies (Abe, 2009; Christ et al., 2009; Gamer et al., 2009; Ganis et al., 2009; Kozel et al., 2004), since telling the truth is assumed to be an automatic and default response, the incorrect-lie trials (when participants made incorrect guesses and lied) should involve a greater part of the executive functioning system (e.g., attention, working memory, inhibition, cognitive switching, and planning; Christ et al., 2009; Evans & Lee, 2011) than the incorrect-truth trials (when participants made incorrect guesses and told the truth). Thus, because of the involvement of executive control in lying, incorrect-lie trials should involve more neural resources than the incorrect-truth trials. Existing fMRI studies involving non-spontaneous deception have revealed that lying engenders greater activations in such dorsal prefrontal cortical regions as the left SFG (Abe et al., 2009; Abe,

Suzuki, Mori, Itoh, & Fujii, 2007; Lee, Lee, Raine, & Chan, 2010; Phan et al., 2005; Priori et al., 2008), which is measurable by the fNIRS methodology (Tian, Sharma, Kozel, & Liu, 2009). Thus, we hypothesized that lying about one's incorrect predictions in our guessing game would produce a greater level of neural activations in the left SFG than truth-telling about incorrect predictions. Furthermore, the existing fMRI studies suggest that the prefrontal regions are the cortical part of the reward network that is responsive to rewards associated with success (McClure, Laibson, Loewenstein, & Cohen, 2004; O'Doherty, 2004; Rademacher et al., 2010; Schultz, 2006). They involve the DLPFC, ventrolateral prefrontal cortex (VLPFC), and orbitofrontal cortex (OFC). Of the cortical part of the reward network, activities in such frontal areas as the middle frontal gyrus (MFG) and SFG (McClure et al., 2004; Pochon et al., 2002; Spielberg et al., 2011) are measurable by the fNIRS methodology. Thus, we hypothesized that because truth-telling about incorrect predictions would reveal failure whereas truth-telling about correct predictions would reveal success, the latter would produce greater neural activities in such frontal areas as the MFG and SFG than the former.

2. Method

2.1. Participants

Twenty-four healthy volunteers participated in the present study. Two were excluded due to procedural errors. All participants but four lied due to the highly motivating nature of our paradigm, which allowed us to compare specifically the lies and truths told by the same participants as in previous neural imaging studies of deception (e.g., Lee et al., 2002). In the end, there were 18 valid participants (7 males, 11 females, 19–23 years old, mean age = 21.00 years and $SD = 1.33$ years). All participants had normal or corrected to normal vision and were right-handed. None had a history of any neurological or psychiatric disorder. The research was

approved by the university ethics committee. The participants gave informed consent prior to their participation in the study.

2.2. Procedure

Participants were tested individually, seated in front of a computer screen, with an experimenter present in a quiet room. Before the game, participants were told that a coin would appear on either the left or the right side of the screen and were instructed to guess which side of the screen the coin would appear on by moving their corresponding hand. Participants put each of their hands in one of the two drawers of a desk so their hand movements would not be directly visible to the experimenter. Participants were then told that after they made their guess by moving one of their hands and the coin had appeared on the right or left side of the screen, a message would come up on the screen asking them whether they guessed the location of the coin correctly ("Is your guess correct or not?"). They then responded verbally "correct" or "incorrect" when the word "respond" appeared on the screen. At this point, the experimenter recorded the response without knowing if the participant was telling a lie or the truth.

We told the participants that a coin would appear on either side of the screen according to an implicit complex rule. Actually, unbeknownst to the participants, the location of the coin was controlled by a computer program so that only 1/3 of the time the coin would appear on the side predicted by the participants. In other words, the side where the coin in a particular trial would appear was contingent on the participants' prediction in that trial. If participants responded honestly on all trials, they would guess incorrectly substantially more frequently than they would guess correctly and therefore would have to endure a prolonged experimental session.

The participants would receive or lose points according to their self-reported accuracy. They would gain 10 points only if they said they predicted correctly; otherwise they would lose 10 points. Participants were told that they could have a rest after one block (12 trials) and the game would not end unless they had gained 100 points at the end of the block. Otherwise they would have to continue to guess in next 12 trials. Since the probability for a correct guess was lower than for an incorrect guess, participants would be highly motivated to make deceptive responses to gain points in order to end the game. However, unbeknownst to participants, the experiment would end after 120 trials. Also, unbeknownst to participants, we installed hidden cameras inside the drawers to record the movement of individuals' hands. Additional hidden cameras also recorded their face and the screen display of the computer simultaneously (see Fig. 1(a)).

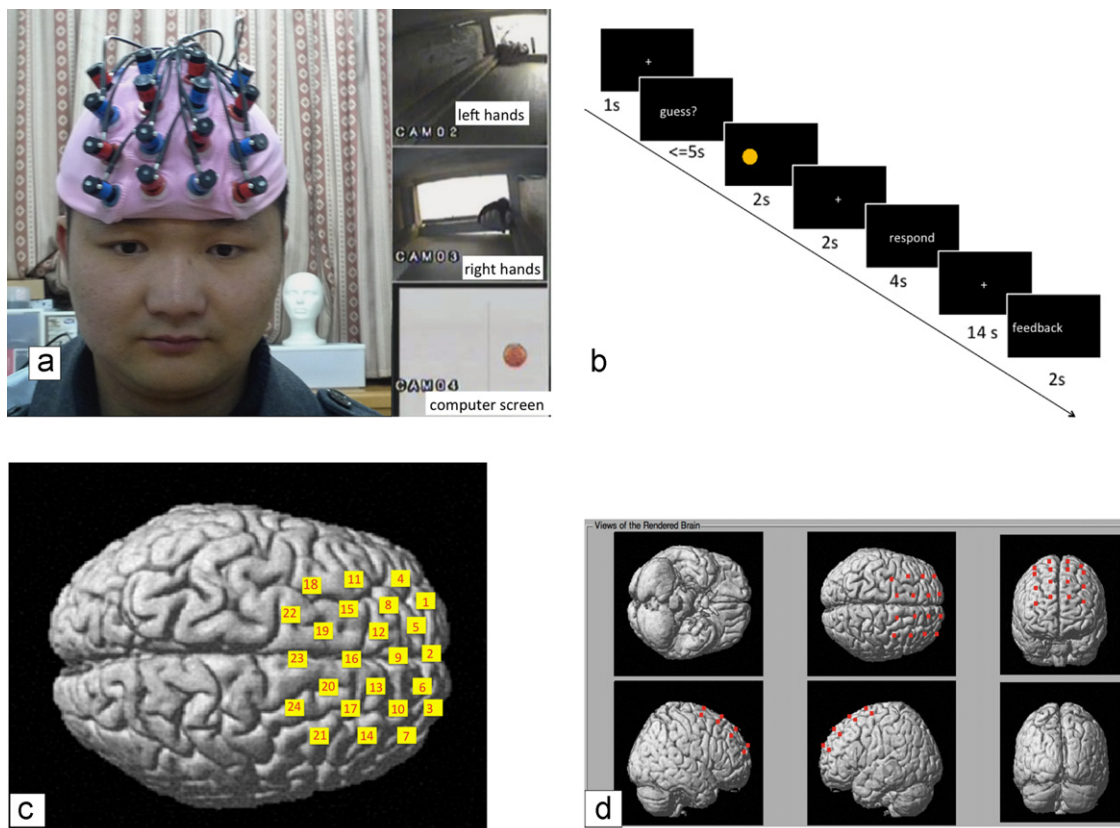


Fig. 1. (a) The experimental video-recording system setup. (b) An example of a guessing trial. (c and d) The estimated cortical locations of the 24 NIRS channels.

E-prime 1.2 was used to present the stimulus. The entire experiment consisted of a minimum of 24 trials to a maximum of 120 trials. Each trial began with the presentation of the fixation cross (1 s), followed by the guessing instruction in the form of a picture, “guess” (2 s), after which a coin would appear either on the right or left side of the screen (see Fig. 1(b)). Participants were instructed to verbally respond “correct” or “incorrect” depending on whether they guessed correctly or incorrectly each time that the “response” instruction appeared on the screen. Then, the total cumulative score they had obtained thus far would be displayed on the screen.

Upon completion of the testing session, all participants were debriefed. Debriefing included telling participants about the purpose of the study, the general findings of previous studies with similar procedures, and an opportunity to view the hidden cameras. All participants received RMB 20 for participating in the study.

2.3. Data acquisition

A 24 channel continuous wave system (ETG-4000, Hitachi Medical Co., Japan) was used in the present study. The probes of the NIRS machine were fixed using one 9×9 cm² rubber shell over the frontal areas. The shell was covered with a nylon-net to keep it attached to the head. The shell of 16 probes, consisting of a 4×4 array with eight light emitters and eight detectors, was capable of measuring the relative concentrations of hemoglobin at 24 points (see Fig. 1(c) and (d)). The inter-optode distance was 30 mm, which allowed for the measurement of neural activities approximately 15–25 mm beneath the scalp. Optical data from individual channels were collected at two different wavelengths (695 and 830 nm) and analyzed using the modified Beer–Lambert Law for a highly scattering medium (Cope & Delpy, 1988). Changes in [oxy-Hb] and [deoxy-Hb] signals were calculated in units of millimolar–millimeter (mM \times mm) (Maki et al., 1995). The sampling rate was set to 10 Hz.

The placements of the probes in the bilateral dorsal frontal areas were based on our hypotheses derived from the existing related studies (Abe et al., 2009; Abe et al., 2007; Lee, Lee, Raine, & Chan, 2010; Phan et al., 2005; Priori et al., 2008; Tian et al., 2009). To ensure probe placement consistency across participants, we placed the lowest probes along the Fp1–Fp2 line in accordance with the international 10–20 system for electroencephalography. A 3D digitizer (EZT-DM401, Hitachi Medical Corporation, Japan) was then used to measure the exact spatial location of each optode in relation to the veridical landmarks of a participant’s head (i.e., nasion, inion, Cz, the pre auricular points anterior to the left and right ears). Using the algorithms by Singh, Okamoto, Dan, Jurcak, and Dan (2005), we converted the 3D spatial location data obtained from the 3D digitizer to obtain cortical positions of our NIRS channels on an estimated MNI space. The NIRS channels covered a large swath of the dorsal prefrontal cortex including the right and left middle and superior frontal gyri (Brodmann’s Areas 6, 8, 9, 10, 46).

2.4. Data analysis

We analyzed the [oxy-Hb] and [deoxy-Hb] signals. For each participant, we segmented event epochs from the time course data. Each event epoch consisted of a 2 s period prior to stimulus onset (which was when the message “respond” appeared on the screen), 14 s of the stimulus and recovery period, and a 2 s post-stimulus period.

2.4.1. General linear model (GLM) analysis

To explore the spatial correlates underlying the different trial types, the [oxy-Hb] and [deoxy-Hb] signals data were analyzed using NIRS-SPM. The NIRS-SPM toolbox enables the NIRS data to be statistically analyzed based on the GLM. The GLM allows us to control some of the extraneous factors such as drift, movements, and heartbeats. More importantly, this analysis also allows us to test various effects independently (i.e., the contrast between incorrect-lie and incorrect-truth, and between incorrect-truth and correct-truth; Jang et al., 2009; Tak et al., 2011; Ye, Tak, Jang, Jung, & Jang, 2009). For all these contrasts, we used the data from the same 18-s trial epoch. For each participant, data were preprocessed to remove sources of noise and artifact (such as movement and heart rate) using a hemodynamic response function (hrf) filter and a wavelet-MDL (minimum description length) detrending algorithm. Then, a general linear model incorporating task effects, a mean and a linear trend were used to compute parameter estimates (beta values of the GLM model as the weights) and *t*-contrasts for two comparisons (incorrect-lie minus incorrect-truth, and incorrect-truth minus correct-truth) at each channel. To control for false positives, all *p*-values were corrected by false discovery rate ($FDR < .05$; Singh & Dan, 2006).

2.4.2. Time course waveform analysis

Because we used a slow-event related design, we were able to obtain the time courses of the grand averaged incorrect-lie, incorrect-truth, and correct-truth trials, respectively. As described above, each event epoch consisted of a 2 s period prior to stimulus onset (which was when the message “respond” appeared on the screen), a 14 s stimulus and recovery period, and a 2 s post-stimulus period.

Several steps were required to conduct the analysis using the raw time series data: to remove baseline drifts and pulsation due to the heartbeat, the raw hemoglobin continuous data was filtered by a high-pass filter of 0.01 Hz and a low-pass filter of 0.3 Hz. Then, the baseline was calculated by the least squares model fitting procedure according to the activities in the pre-stimulus and post-stimulus period. For each epoch of each channel, a first-degree baseline fit to the mean of the 2 s pre-stimulus and 2 s post-stimulus periods was performed. After baseline correction, we computed the mean and the standard deviation of each channel for each participant and converted the raw time course values to *Z* scores. The formula is as below:

$$Z = \frac{(X - M)}{S}$$

where *X* is the raw time courses value of the changes in [oxy-Hb] or [deoxy-Hb] after baseline correction in each epoch, *M* is the mean value of the whole time course of each subject for this channel, and *S* is the standard deviation of each subject for this channel. Then we averaged all the event epochs for the channel of a particular trial type to derive a grand averaged time course wave form of the channel for the trial type, and extracted the amplitude and peak latency of the mean time course of each trial type. We calculated the time courses of each channel based on the significant results of the GLM analyses (after *FDR* correction to control for false positives).

2.4.3. Functional connectivity cross-correlation analysis

The GLM results only provide information about which areas showed significant increases in activity during the task. However, during deception, these brain regions do not act in isolation. To explore how regions of the brain communicate with one another during specific cognitive processes involved in spontaneous deception, we used a cross-correlation analysis to evaluate the function connectivity between a seed channel and other channels along the time course of the trial events. Such interactions have typically been characterized by identifying regions that show correlated fluctuations in their fNIRS time series data, with the assumption that temporal correlations in hemoglobin signal might reflect synchronous neural activities in the communicating regions (Rissman, Gazzaley, & D’Esposito, 2004). The seed channel was chosen according to the significant results from the above GLM analysis.

To examine whether the time-dependent neural activities of the seed channel influenced the neural activities of another channel (the target channel), we first subtracted the [oxy-Hb] or [deoxy-Hb] time course waveform of one trial type of the seed channel (e.g., the incorrect-lie trial) from that of another trial type (e.g., incorrect-truth trial) of the same seed channel. We did the same to the data from the target channel. Then, we calculated Pearson correlations between the time course difference values in time windows spanning 5 s (50 sample points) on the seed channel and a 5 s moving time window on the target channel. Because the hemodynamic response function (HRF) lasts for about 15 s per epoch, and our slow event-related design was able to capture the entire time course, we used to the 5 s moving window to capture the coherences between the seed and target channels in terms of the initial rise, the peaking, and the later decline of the HRF.

We then estimated the effect of time lag by shifting the time window on the target channel in consecutive steps of 0.1 s. For each step of time shift, the correlation coefficient between the time windows of the seed channel and the target channel was calculated as a numerical measure of coherence. Then we transformed the *r*-value into a *z*-value according to the Fisher transformation and displayed the result within a heat map (the time courses of the seed channel as the *x*-axis and the *y*-axis representing the time lag). All *p*-values were corrected by false discovery rate to control for false positives ($FDR < .001$). To examine whether the influence of the seed channel on the target channel was bidirectional, we performed the same cross-correlation analysis with the above seed channel as the target channel and the above target channel as the seed channel.

We performed the above analyses between the seed channel and each of the other channels. We did so for the [oxy-Hb] and [deoxy-Hb] data, respectively.

2.4.4. Correlational analyses between behavior and NIRS data

To identify neural activity associated with participants’ deceptive behaviors, we conducted correlation analyses between deceptive behaviors and NIRS data. Participants’ deceptive behaviors were measured in two ways. First, because different participants might begin to lie at different time points, we used the first incorrect-lie trial (FIT) to index such initiation of lying. Second, we obtained an incorrect-lie rate for each participant based on the percent of trials the participant reported “correct” when they in fact predicted incorrectly divided by the total number of trials they predicted incorrectly. Pearson’s correlation coefficients between the behavioral measures and NIRS data for each channel based on the results of the GLM analyses were calculated. All *p*-values were corrected by false discovery rate to control for false positives ($FDR < .05$).

3. Results

3.1. Behavioral data

Eighteen participants took part in 86 trials on average (ranging from 36 trials to 120 trials, $SD=33$), including 10.56 trials of incorrect-lie on average ($SD=5.95$), 36 trials of incorrect-truth on average ($SD=22.12$), and 20.44 trials of correct-truth on average ($SD=10.78$). The mean FIT was the 28.2th (ranging from 1st to 108th trial, $SD=32.87$ th). The average incorrect-lie rate was 27.55% (ranging from 4.41% to 50.00%, $SD=15.16\%$).

3.2. NIRS results

3.2.1. Spatial correlates of deception

To investigate the spatial correlates of deception, we compared the hemodynamic activities between the incorrect-lie and incorrect-truth trials, as well as between the correct-truth and incorrect-truth trials. The results are shown in Table 1. Specifically, the incorrect-lie trials elicited significantly larger changes in [oxy-Hb] concentration than the incorrect-truth trials in Channel 15 (BA8, left SFG). This finding suggests that when participants predicted incorrectly and lied, it engendered significantly more [oxy-Hb] activities in this left frontal area than when they admitted their incorrect prediction. Other than this significant effect, this contrast produced no other significant [oxy-Hb] and [deoxy-Hb] changes in the 24 channels.

However, when different types of truth-telling trials were contrasted, more channels were significant. The correct-truth (honest success) trials elicited significantly larger [oxy-Hb] changes in Channel 20 (BA8, right SFG) than the incorrect-truth (honest failure) trials. The correct-truth trials also elicited significantly larger [deoxy-Hb] changes in Channel 11 (BA9, left MFG) than the incorrect-truth trials.

3.2.2. Time course waveform of deception

To further explore the potential differences between these different types of trials, we also extracted the peak amplitudes and latencies of the mean [oxy-Hb] and [deoxy-Hb] signal waveforms of each participant in each type of trial in each channel. When we compared these measures between trial types, the paired t test results showed that there was only a significant difference in the peak amplitude of [oxy-Hb] signals between correct-truth trials and incorrect-truth trials in Channel 20 (BA8, right SFG) ($t(17)=3.11$, $p<.01$): the correct-truth trials elicit significantly higher peak amplitude than the incorrect-truth trials (see Fig. 2). There were no significant differences in the peak amplitude or latency of [oxy-Hb] or [deoxy-Hb] signals between incorrect-lie trials and incorrect-truth trials (see Fig. 3).

Table 1

The paired t -test results about beta value of the hemodynamic activities based on the GLM analyses.

Ch	Estimated MNI			Brain area	Probability	Paired t -test	
	X	Y	Z			Oxy	Deoxy
Incorrect-lie minus incorrect-truth							
Ch15	-22	25	63	L superior frontal gyrus (BA8)	.95	2.43*	NS
Correct-truth minus incorrect-truth							
Ch11	-35	31	51	L middle frontal gyrus (BA9)	.95	NS	4.81*
Ch20	15	18	69	R superior frontal gyrus (BA8)	1.00	2.76*	NS

* Note: The results are corrected by $FDR < .05$, and NS represents non-significant.

3.2.3. The functional connectivity analysis results

To examine the functional connectivity of the processes of lying vs. truth-telling, cross-correlational analyses were conducted. We used the time courses of the contrast data between the incorrect-lie and incorrect-truth trials of Channel 15 as the seed channel because the GLM analyses showed this channel to be the only significant one for the contrast. The results (with FDR corrections) showed that there was significant functional connectivity between the time courses of [oxy-Hb] change extracted from the seed Channel 15 (BA8, left SFG) and the target Channel 1 (BA10, left MFG). Fig. 4 shows that the [oxy-Hb] activity differences between incorrect-lie trials and incorrect-truth trials of the initial 0–2 s from Channel 15 were significantly associated with those in Channel 1, and further there was also about a 0.5 s time lag in the [oxy-Hb] activities in Channel 1 relative to those in Channel 15. However, when we used Channel 1 as the seed and Channel 15 as the target, no significant results were obtained. Thus, it appeared that the [oxy-Hb] activity differences in Channel 1 were influenced by the [oxy-Hb] activity initiated in Channel 15.

When we used the [deoxy-Hb] differences between the incorrect-lie and incorrect truth trials in Channel 15 to cross-correlate with those in the rest of channels, no significant associations were found in both directions.

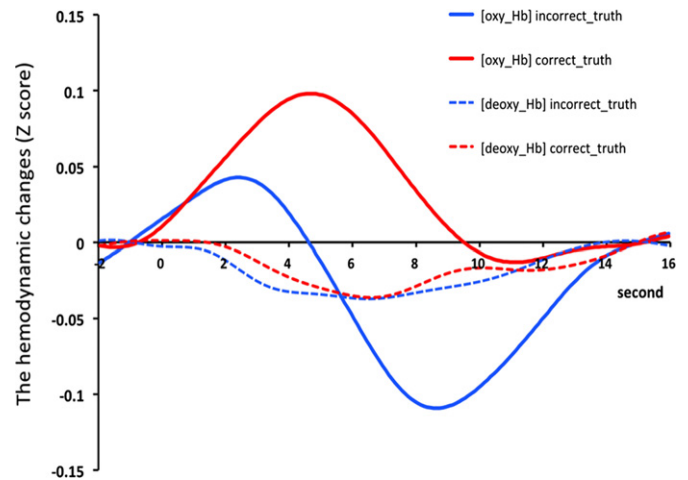


Fig. 2. The time courses of the mean [oxy-Hb] and [deoxy-Hb] changes (z score) of the correct-truth trials and incorrect-truth trials in Channel 20 (BA 8, the right superior frontal gyrus).

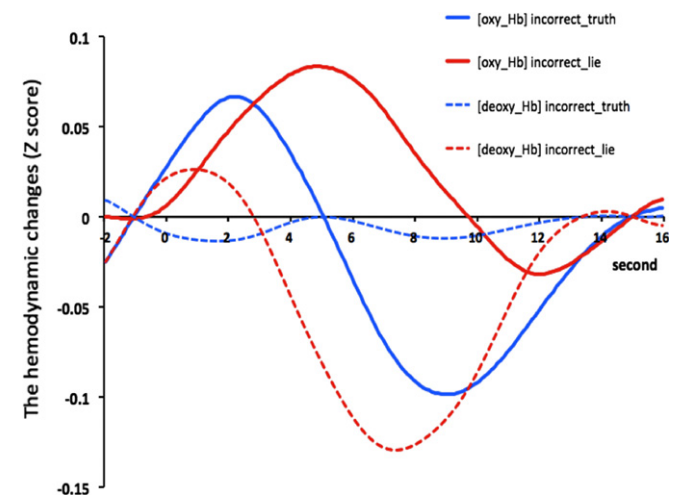


Fig. 3. The time courses of the mean [oxy-Hb] and [deoxy-Hb] changes (z score) of the incorrect-lie trials and incorrect-truth trials in Channel 15 (BA 8/9, the left superior frontal gyrus).

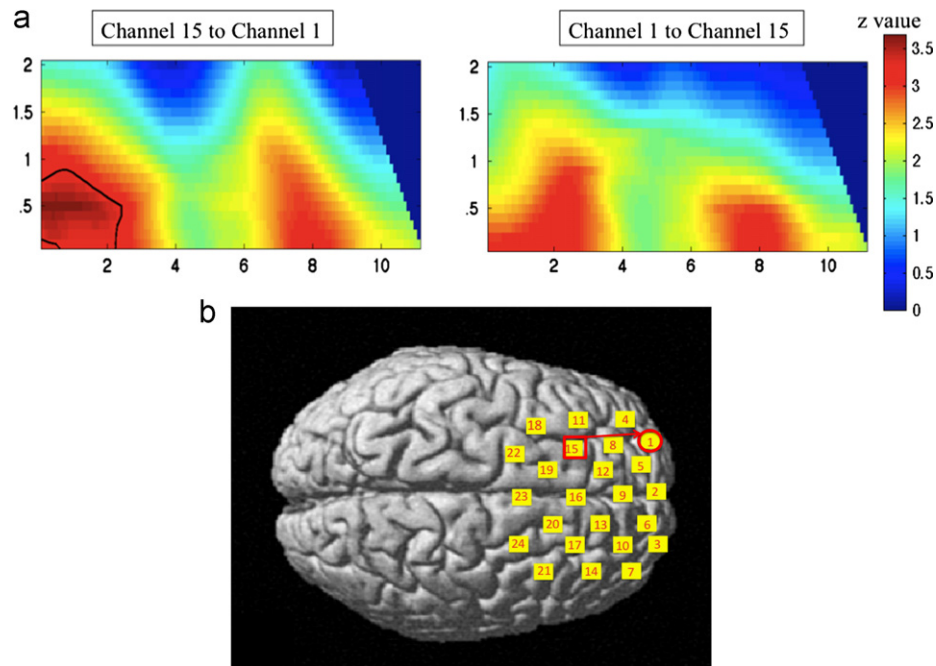


Fig. 4. (a) Statistical z-map showing the significant functional connectivity between time course results of the [oxy-Hb] activity differences between the incorrect-lie and incorrect-truth trials of Channel 15 and those of Channel 1. The x-axis represents the time courses of the seed channel and the y-axis represents the time lag of the target channel relative to each time point of the seed channel. The left panel shows the results when the seed channel was Channel 1. The p -value was corrected by FDR < .001. Significant associations are marked by a black line. (b) The cortical locations of the functional connectivity between time course results of the [oxy-Hb] activity differences between the incorrect-lie and incorrect-truth trials of Channel 15 and those Channel 1 based on the estimated cortical coordinates of the 24 NIRS channels.

3.3. The correlation between behavior and NIRS data

3.3.1. Incorrect-lie trials vs. incorrect-truth trials

Pearson correlation analyses showed that neither the FIT nor incorrect-lie rate was significantly correlated with the contrast [oxy-Hb] or [deoxy-Hb] signals between incorrect-lie trials and incorrect-truth trials.

3.3.2. Correct-truth trials vs. incorrect-truth trials

Pearson correlation analyses showed that the differences in the [oxy-Hb] activity between the correct-truth and incorrect-truth trials in Channel 20 (BA8, right SFG) were significantly correlated with FIT ($r = .483$, $p < .05$) (Fig. 5). No other contrasts in the [oxy-Hb] and [deoxy-Hb] activities were significant (including the contrasts between the incorrect-lie and incorrect truth trials). Thus, the hemodynamic response differences between the different types of truth trials but not those between lying and truth-telling trials significantly predicted the first trial where participants told the first lie. More specifically, the larger the differences in the [oxy-Hb] activity between the correct-truth (i.e., success) and incorrect-truth (i.e., failure) trials were, the earlier participants decided to lie.

4. Discussion

The present study examined the neural correlates of spontaneous deception. Specifically, with a paradigm modeled after Greene and Paxton (2009), we investigated whether neural activities would differ between the trials where individuals spontaneously lied and the trials where the same individuals spontaneously told the truth when they guessed incorrectly. We specifically focused on whether spontaneous deception would engage a network of neural regions similar to that found in studies where participants were instructed to lie. Further, we tested hypotheses about the reward system involved in deception, specifically whether there were different brain activity patterns

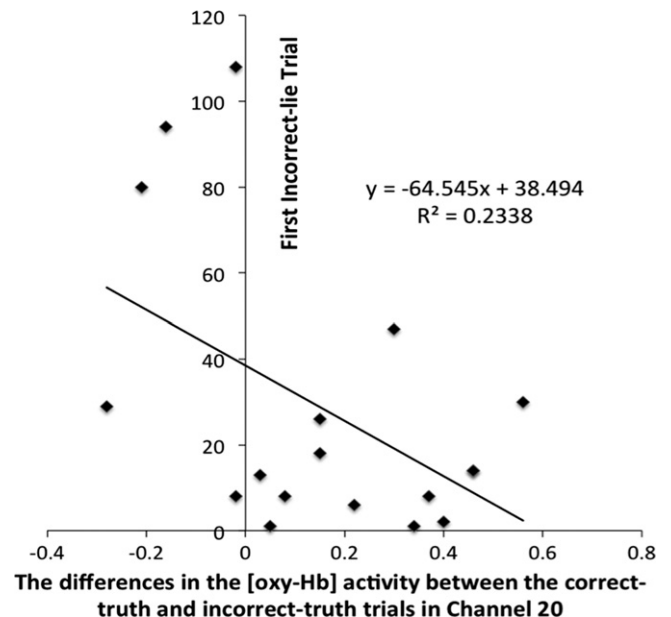


Fig. 5. The scatters plot of the correlation between deceptive behavior and NIRS data.

between incorrect-truth trials revealing failure and correct-truth trials revealing success.

4.1. Incorrect-lie trials vs. incorrect-truth trials

Consistent with our hypothesis, incorrect-lie trials elicited significantly greater [oxy-Hb] changes in the left SFG, relative to incorrect-truth trials. This finding derived from spontaneous deception is generally consistent with previous fMRI findings

that have also shown greater blood oxygenation level dependent (BOLD) signal changes in the dorsal prefrontal cortex in general and the left SFG specifically when participants were instructed to tell a lie rather than when they were instructed to tell the truth (Christ et al., 2009; Gamer et al., 2009; Kozel et al., 2004; Lee et al., 2002; Spence et al., 2001). Thus, despite perennial criticism that existing studies using instructed deception paradigms lack ecological validity due to the “unnaturalistic” and artificial nature of these paradigms, the results of those studies appear highly congruent with our findings for spontaneous deception.

Our functional connectivity results revealed that there is a significant temporal coherence between Channel 15 (BA8, left SFG) and Channel 1 (BA10, left MFG), with the peak coherence having about 0.5 s delay in Channel 1 relative to Channel 15. However, the temporal coherence from Channel 1 to Channel 15 was not significant. This temporal coherence cannot be explained by a vascular concentration change spreading from Channel 15 (BA8) to Channel 1 (BA10). Channel 15 (BA8) is located on the posterior lateral prefrontal cortex, and Channel 1 (BA10) is located on the anterior prefrontal cortex. If this temporal coherence was caused by vascular spreading, there should have been significant temporal coherences between Channel 15 (BA8) and its nearest channels, which was not the case. Thus, this temporal coherence from Channel 15 (BA8) to Channel 1 (BA10) was likely due to the underlying functional neural connectivities between the two cortical areas. One explanation for this temporal coherence is that both areas (the left SFG (BA8) and MFG (BA10)) are essential in executive functioning. Specifically, the left SFG (BA8) is a key area involved in working memory (du Boisgueheneuc et al., 2006; Johnson, Raye, Mitchell, Greene, & Anderson, 2003) and the left MFG (BA10) is strongly activated during task switching (Kim, Cilles, Johnson, & Gold, 2012). It is possible that during the incorrect-lie trials, after the truth was inhibited, participants needed to recruit the network of task switching to generate an alternative response (a lie). These cognitive activities might have engendered the neural coherences between the two cortical regions manifested in a unidirectional fashion. Our finding thus provides a new piece of evidence to support the theory that spontaneous lying, like instructed lying, involves more cognitive processes than truth-telling because it calls for the use of both working memory and task switching.

4.2. Correct-truth trials (success) vs. incorrect-truth trials (failure)

Consistent with our hypothesis, we found that the correct-truth (honest success) trials produced greater [oxy-Hb] signals in Channel 20 (BA8, right SFG) and greater [deoxy-Hb] signals in Channel 11 (BA9, left MFG) than the incorrect-truth (honest failure) trials. Further, consistent with the GLM results, when we examined the time courses of the mean [oxy-Hb] signal changes for the correct-truth and incorrect-truth trials, we found that the correct-truth trials elicited significantly higher peak amplitudes of [oxy-Hb] signal changes than the incorrect-truth trials in Channel 20 (BA8, right SFG; Fig. 2).

One possibility for this result was that the correct-truth trials represented the situations when participants gained points, or succeeded, whereas the incorrect-truth trials represented the situations when participants lost points, or failed. The participants had to earn enough points to stop the seemingly boring game sooner. Therefore, the points served as a reinforcer. Also, participants were told that they could not receive the participation fee until they had finished. Thus, participants were sufficiently motivated to try and gain points and to avoid losing points. The heightened activity in the frontal area (right SFG and left MFG) might reflect the involvement of the reward system.

Previous studies have identified that many prefrontal areas are sensitive to reward (Haber & Knutson, 2010; Wallis & Miller, 2003). The right SFG (BA8) and left MFG (BA9) have been found to be the areas that are not only activated by the cognitive aspects of tasks but also modulated by positive reward values (Pochon et al., 2002; Spielberg et al., 2011). In the present task, correct-truth trials led to gaining points while incorrect-truth trials led to losing points, although in both trials participants were telling the truth, so that cortical regions of the “reward” network might have been activated differentially, resulting in the correct-truth trials producing greater [oxy-Hb] signals in Channel 20 (BA8, right SFG) and greater [deoxy-Hb] signals in Channel 11 (BA9, left MFG) than the incorrect-truth trials.

4.3. Behavioral and neural correlates

We did not find that the [oxy-Hb] signal differences between incorrect-lie and incorrect-truth trials were significantly correlated with the first incorrect-lie trial (FIT) nor the incorrect-lie rate. These null findings may suggest that neural activity differences between the lie-telling trials and truth-telling trials were not likely the basis of when participants first decided to lie or how frequently they would subsequently lie.

However, interestingly, we found that the [oxy-Hb] signal contrast between the correct-truth and incorrect-truth trials was significantly correlated negatively with the first incorrect-lie trial (FIT). More specifically, as participants' hemodynamic response difference between the correct-truth trials and the incorrect-truth trials increased, they initiated their first lie earlier. Note that the differences between these two types of trials were between guessing correctly and receiving points (success), and guessing incorrectly and losing points (failure). Thus, it appeared that the greater the neural response differences between receiving points and losing points, the sooner participants began lying. However, because the same neural response differences did not correlate significantly with the participants' rate of lying, once participants started lying, their differential valuations of gaining and losing points were no longer a factor for how frequently they would lie. Our findings provided evidence that the neural activity difference may mediate individuals' actual deceptive behaviors (Karim et al., 2010).

5. Limitations

Due to the limitation of the cortical depth that the NIRS signal can be detected by the optical detectors on the scalp, we could only assess the cortical regions involved in spontaneous deception that are close to the cortical surface. For this reason, we were unable to examine the roles of some important brain areas such as the ACC, amygdala, and striatum. Specifically, previous studies have found that the ACC plays an important part in monitoring cognitive conflict in the context of deception (Abe et al., 2006; Kozel et al., 2004; Langleben et al., 2002). However, due to the limitation of NIRS, our study could not assess its role in spontaneous deception.

Also due to the same limitation, we could not assess the role of the subcortical regions involved in the reward system when participants gained or lost points in the incorrect-truth, incorrect-lie, and correct-truth trials. Previous research has found that when receiving rewards, there is a sustained recruitment of the striatum, nucleus accumbens (NACC), ventral tegmental area (VTA) and ventromedial prefrontal cortex (VMPFC) (de Greck et al., 2008; Izuma, Saito, & Sadato, 2008; McClure et al., 2004; Rademacher et al., 2010). In addition, due to the limited number of optodes (24 channels) that we could use, neural activities in

some cortical regions not covered by these channels were unfortunately missed. Thus, future fMRI studies are needed to replicate and extend the current findings and to uncover other important cortical and subcortical regions involved in spontaneous deception.

In addition, there is also a limitation to our paradigm. In the present paradigm, participants were motivated to deceive by a negative reinforcement (i.e., stopping the boring game sooner). Although participants did receive positive reinforcement in the form of a participation fee, this payment was given regardless of their performance. Future studies may wish to modify our paradigm such that participants will gain positive rewards (e.g., monetary points) when gaining points so as to examine whether the present findings regarding the reward network could be replicated.

6. Summary

The present study focused on the neural correlates underlying spontaneous deception. We used the near-infrared spectroscopy (NIRS) methodology to investigate the neural responses in a guessing game modeled after Greene and Paxton (2009). We found that when compared to truth-telling, spontaneous deception, like instructed deception, engenders greater involvement of such prefrontal regions as the left superior frontal gyrus. We also found that the correct-truth trials produced greater neural activities in the left middle frontal gyrus and right superior frontal gyrus than the incorrect-truth trials, suggesting the involvement of the reward system. Furthermore, the present study confirmed the feasibility of using NIRS to study spontaneous deception.

Taken together, these results provide new evidence to support the idea that spontaneous deception shares some similarities with instructed deception: spontaneous deception also needs to recruit more neural resources than telling the truth. To lie, individuals need to inhibit the truth while generating an alternative response (a lie). The role of the reward system in the process of spontaneous deception should also be considered. As suggested by the present findings, it appears that one's decision to decide to tell the truth or a lie entails positive or negative consequences, and such consequences in turn may affect whether and when one decides to lie. It is thus necessary to incorporate the reward system into the existing deception models. The revised models may not only account more fully for the existing behavioral and neural findings but may also make novel predictions for future behavioral and neural imaging studies. Furthermore, the present study confirmed the feasibility of using NIRS to study deception.

References

- Abe, N. (2009). The neurobiology of deception: evidence from neuroimaging and loss-of-function studies. *Current Opinion in Neurology*, 22(6), 594–600, <http://dx.doi.org/10.1097/WCO.0b013e3283323c3f>.
- Abe, N. (2011). How the brain shapes deception: an integrated review of the literature. *The Neuroscientist*, 17, 560–574, <http://dx.doi.org/10.1177/1073858410393359>.
- Abe, N., Fujii, T., Hirayama, K., Takeda, A., Hosokai, Y., Ishioka, T., et al. (2009). Do parkinsonian patients have trouble telling lies? The neurobiological basis of deceptive behaviour. *Brain*, 132(5), 1386, <http://dx.doi.org/10.1093/brain/awp052>.
- Abe, N., Okuda, J., Suzuki, M., Sasaki, H., Matsuda, T., Mori, E., et al. (2008). Neural correlates of true memory, false memory, and deception. *Cerebral Cortex*, 18(12), 2811–2819, <http://dx.doi.org/10.1093/cercor/bhn037>.
- Abe, N., Suzuki, M., Mori, E., Itoh, M., & Fujii, T. (2007). Deceiving others: distinct neural responses of the prefrontal cortex and amygdala in simple fabrication and deception with social interactions. *Journal of Cognitive Neuroscience*, 19(2), 287–295, <http://dx.doi.org/10.1162/jocn.2007.19.2.287>.

- Abe, N., Suzuki, M., Tsukiura, T., Mori, E., Yamaguchi, K., Itoh, M., et al. (2006). Dissociable roles of prefrontal and anterior cingulate cortices in deception. *Cerebral Cortex*, 16(2), 192–199, <http://dx.doi.org/10.1093/cercor/bhi097>.
- Christ, S. E., Van Essen, D. C., Watson, J. M., Brubaker, L. E., & McDermott, K. B. (2009). The contributions of prefrontal cortex and executive control to deception: evidence from activation likelihood estimate meta-analyses. *Cerebral Cortex*, 19(7), 1557–1566, <http://dx.doi.org/10.1093/cercor/bhn189>.
- Cope, M., & Delpy, D. T. (1988). System for long-term measurement of cerebral blood and tissue oxygenation on newborn infants by near infra-red transillumination. *Medical & Biological Engineering & Computing*, 26(3), 289–294, <http://dx.doi.org/10.1007/BF02447083>.
- Crossman, A. M., & Lewis, M. (2006). Adults' ability to detect children's lying. *Behavioral Science and the Law*, 24(5), 703–715, <http://dx.doi.org/10.1002/bsl.731>.
- de Greck, M., Rotte, M., Paus, R., Moritz, D., Thiemann, R., Proesch, U., ... et al. (2008). Is our self based on reward? Self-relatedness recruits neural activity in the reward system. *NeuroImage*, 39 (4), 2066–2075. [10.1016/j.neuroimage.2007.11.006](http://dx.doi.org/10.1016/j.neuroimage.2007.11.006).
- DePaulo, B. M., Lindsay, J. J., Malone, B. E., Muhlenbruck, L., Charlton, K., & Cooper, H. (2003). Cues to deception. *Psychological Bulletin*, 129(1), 74–118, <http://dx.doi.org/10.1037/0033-2909.129.1.74>.
- du Boisgueheneuc, F., Levy, R., Volle, E., Seassau, M., Duffau, H., Kinkingnehun, S., et al. (2006). Functions of the left superior frontal gyrus in humans: a lesion study. *Brain*, 129, 3315–3328, <http://dx.doi.org/10.1093/brain/awl244>.
- Evans, A. D., & Lee, K. (2011). Verbal deception from late childhood to middle adolescence and its relation to executive functioning skills. *Developmental Psychology*, 47(4), 1108–1116, <http://dx.doi.org/10.1037/a0023425>.
- Fassbender, C., Murphy, K., Foxe, J. J., Wylie, G. R., Javitt, D. C., Robertson, I. H., et al. (2004). A topography of executive functions and their interactions revealed by functional magnetic resonance imaging. *Cognitive Brain Research*, 20(2), 132–143, <http://dx.doi.org/10.1016/j.cogbrainres.2004.02.007>.
- Fu, G. Y., & Lee, K. (2007). Social grooming in the kindergarten: the emergence of flattery behavior. *Developmental Science*, 10(2), 255–265, <http://dx.doi.org/10.1111/j.1467-7687.2007.00583.x>.
- Gamer, M., Klimecki, O., Bauermann, T., Stoeter, P., & Vossel, G. (2009). fMRI-activation patterns in the detection of concealed information rely on memory-related effects. *Social Cognitive and Affective Neuroscience*, <http://dx.doi.org/10.1093/scan/nsp005>.
- Ganis, C., Kosslyn, S. M., Stose, S., Thompson, W. L., & Yurgelun-Todd, D. A. (2003). Neural correlates of different types of deception: an fMRI investigation. *Cerebral Cortex*, 13(8), 830–836, <http://dx.doi.org/10.1093/cercor/13.8.830>.
- Ganis, C., Morris, R. R., & Kosslyn, S. M. (2009). Neural processes underlying self-and other-related lies: an individual difference approach using fMRI. *Social Neuroscience*, 4(6), 539–553, <http://dx.doi.org/10.1080/17470910801928271>.
- Gombos, V. A. (2006). The cognition of deception: the role of executive processes in producing lies. *Genetic, Social, and General Psychology Monographs*, 132(3), 197–214, <http://dx.doi.org/10.3200/MONO.132.3.197-214>.
- Greene, J. D., & Paxton, J. M. (2009). Patterns of neural activity associated with honest and dishonest moral decisions. *Proceedings of the National Academy of Sciences*, 106(30), 12506–12511, <http://dx.doi.org/10.1073/pnas.0900152106>.
- Haber, S. N., & Knutson, B. (2010). The reward circuit: linking primate anatomy and human imaging. *Neuropsychopharmacology*, 35(1), 4–26, <http://dx.doi.org/10.1038/npp.2009.129>.
- Izuma, K., Saito, D. N., & Sadato, N. (2008). Processing of social and monetary rewards in the human striatum. *Neuron*, 58, 284–294, <http://dx.doi.org/10.1016/j.neuron.2008.03.020>.
- Jang, K. E., Tak, S., Jung, J., Jang, J., Jeong, Y., & Ye, J. C. (2009). Wavelet minimum description length detrending for near-infrared spectroscopy. *Journal of Biomedical Optics*, 14(3), 034004, <http://dx.doi.org/10.1117/1.3127204>.
- Johnson, M. K., Raye, C. L., Mitchell, K. J., Greene, E. J., & Anderson, A. W. (2003). fMRI evidence for an organization of prefrontal cortex by both type of process and type of information. *Cerebral cortex*, 13(3), 265–273, <http://dx.doi.org/10.1093/cercor/13.3.265>.
- Johnson, R., Barnhardt, J., & Zhu, J. (2004). The contribution of executive processes to deceptive responding. *Neuropsychologia*, 42(7), 878–901, <http://dx.doi.org/10.1016/j.neuropsychologia.2003.12.005>.
- Karim, A. A., Schneider, M., Lotze, M., Veit, R., Sauseng, P., Braun, C., et al. (2010). The truth about lying: inhibition of the anterior prefrontal cortex improves deceptive behavior. *Cerebral Cortex*, 20(1), 205–213, <http://dx.doi.org/10.1093/cercor/bhp090>.
- Kim, C., Cilles, S. E., Johnson, N. F., & Gold, B. T. (2012). Domain general and domain preferential brain regions associated with different types of task switching: a meta-analysis. *Human Brain Mapping*, 33(1), 130–142, <http://dx.doi.org/10.1002/hbm.21199>.
- Kozel, F. A., Padgett, T. M., & George, M. S. (2004). A replication study of the neural correlates of deception. *Behavioral Neuroscience*, 118(4), 852–856, <http://dx.doi.org/10.1037/0735-7044.118.4.852>.
- Langleben, D. D. (2008). Detection of deception with fMRI: are we there yet? *Legal and Criminological Psychology*, 13(1), 1–9, <http://dx.doi.org/10.1348/135532507x251641>.
- Langleben, D. D., Schroeder, L., Maldjian, J. A., Gur, R. C., McDonald, S., Ragland, J. D., et al. (2002). Brain activity during simulated deception: an event-related functional magnetic resonance study. *NeuroImage*, 15(3), 727–732, <http://dx.doi.org/10.1006/nimg.2001.1003>.

- Lee, T. M. C., Lee, T. M. Y., Raine, A., & Chan, C. C. H. (2010). Lying about the valence of affective pictures: an fMRI study. *PLoS One*, 5(8), e12291, <http://dx.doi.org/10.1371/journal.pone.0012291>.
- Lee, T. M. C., Liu, H. L., Tan, L. H., Chan, C. C. H., Mahankali, S., Feng, C. M., et al. (2002). Lie detection by functional magnetic resonance imaging. *Human Brain Mapping*, 15(3), 157–164, <http://dx.doi.org/10.1002/hbm.10020>.
- Lloyd-Fox, S., Blasi, A., & Elwell, C. E. (2010). Illuminating the developing brain: the past, present and future of functional near infrared spectroscopy. *Neuroscience and Biobehavioral Reviews*, 34(3), 269–284, <http://dx.doi.org/10.1016/j.neubiorev.2009.07.008>.
- Maki, A., Yamashita, Y., Ito, Y., Watanabe, E., Mayanagi, Y., & Koizumi, H. (1995). Spatial and temporal analysis of human motor activity using noninvasive NIR topography. *Medical Physics*, 22(12), 1997–2005, <http://dx.doi.org/10.1118/1.597496>.
- McClure, S. M., Laibson, D. I., Loewenstein, G., & Cohen, J. D. (2004). Separate neural systems value immediate and delayed monetary rewards. *Science*, 306(5695), 503–507, <http://dx.doi.org/10.1126/science.1100907>.
- Núñez, J. M., Casey, B. J., Egner, T., Hare, T., & Hirsch, J. (2005). Intentional false responding shares neural substrates with response conflict and cognitive control. *NeuroImage*, 25(1), 267–277, <http://dx.doi.org/10.1016/j.neuroimage.2004.10.041>.
- Osaka, N., Osaka, M., Kondo, H., Morishita, M., Fukuyama, H., & Shibasaki, H. (2004). The neural basis of executive function in working memory: an fMRI study based on individual differences. *NeuroImage*, 21(2), 623–631, <http://dx.doi.org/10.1016/j.neuroimage.2003.09.069>.
- O'Doherty, J. P. (2004). Reward representations and reward-related learning in the human brain: insights from neuroimaging. *Current Opinion in Neurobiology*, 14(6), 769–776, <http://dx.doi.org/10.1016/j.conb.2004.10.016>.
- Phan, K. L., Magalhaes, A., Ziemlewicz, T. J., Fitzgerald, D. A., Green, C., & Smith, W. (2005). Neural correlates of telling lies: a functional magnetic resonance imaging study at 4 T. *Academic Radiology*, 12(2), 164–172, <http://dx.doi.org/10.1016/j.acra.2004.11.023>.
- Pochon, J. B., Levy, R., Fossati, P., Lehericy, S., Poline, J. B., Pillon, B., et al. (2002). The neural system that bridges reward and cognition in humans: an fMRI study. *Proceedings of the National Academy of Sciences*, 99(8), 5669–5674, <http://dx.doi.org/10.1073/pnas.082111099>.
- Priori, A., Mameli, F., Cogiamanian, F., Marceglia, S., Tiriticco, M., Mrakic-Sposta, S., et al. (2008). Lie-specific involvement of dorsolateral prefrontal cortex in deception. *Cerebral Cortex*, 18(2), 451–455, <http://dx.doi.org/10.1093/cercor/bhm088>.
- Rademacher, L., Krach, S., Kohls, G., Irmak, A., Gründer, G., & Spreckelmeyer, K. N. (2010). Dissociation of neural networks for anticipation and consumption of monetary and social rewards. *NeuroImage*, 49(4), 3276–3285, <http://dx.doi.org/10.1016/j.neuroimage.2009.10.089>.
- Rissman, J., Gazzaley, A., & D'Esposito, M. (2004). Measuring functional connectivity during distinct stages of a cognitive task. *NeuroImage*, 23(2), 752–763, <http://dx.doi.org/10.1016/j.neuroimage.2004.06.035>.
- Schultz, W. (2006). Behavioral theories and the neurophysiology of reward. *Annual Review of Psychology*, 57, 87–115, <http://dx.doi.org/10.1146/annurev.psych.56.091103.070229>.
- Singh, A. K., & Dan, I. (2006). Exploring the false discovery rate in multichannel NIRS. *NeuroImage*, 33, 542–549, <http://dx.doi.org/10.1016/j.neuroimage.2006.06.047>.
- Singh, A. K., Okamoto, M., Dan, H., Jurcak, V., & Dan, I. (2005). Spatial registration of multichannel multi-subject fNIRS data to MNI space without MRI. *NeuroImage*, 27(4), 842–851, <http://dx.doi.org/10.1016/j.neuroimage.2005.05.019>.
- Sip, K. E., Roepstorff, A., McGregor, W., & Frith, C. D. (2008). Detecting deception: the scope and limits. *Trends in Cognitive Sciences*, 12(2), 48–53, <http://dx.doi.org/10.1016/j.tics.2007.11.008>.
- Spence, S. A., Farrow, T. F., Herford, A. E., Wilkinson, I. D., Zheng, Y., & Woodruff, P. W. (2001). Behavioural and functional anatomical correlates of deception in humans. *NeuroReport*, 12(13), 2849–2853, <http://dx.doi.org/10.1097/00001756-200109170-00019>.
- Spielberg, J. M., Miller, G. A., Engels, A. S., Herrington, J. D., Sutton, B. P., Banich, M. T., et al. (2011). Trait approach and avoidance motivation: lateralized neural activity associated with executive function. *NeuroImage*, 54(1), 661–670, <http://dx.doi.org/10.1016/j.neuroimage.2010.08.037>.
- Tak, S., Yoon, S. J., Jang, J., Yoo, K., Jeong, Y., & Ye, J. C. (2011). Quantitative analysis of hemodynamic and metabolic changes in subcortical vascular dementia using simultaneous near-infrared spectroscopy and fMRI measurements. *NeuroImage*, 55(1), 176–184, <http://dx.doi.org/10.1016/j.neuroimage.2010.11.046>.
- Talwar, V., & Lee, K. (2008). Social and cognitive correlates of children's lying behavior. *Child Development*, 79(4), 866–881, <http://dx.doi.org/10.1111/j.1467-8624.2008.01164.x>.
- Tian, F., Sharma, V., Kozel, F. A., & Liu, H. (2009). Functional near-infrared spectroscopy to investigate hemodynamic responses to deception in the prefrontal cortex. *Brain Research*, 1303, 120–130, <http://dx.doi.org/10.1016/j.brainres.2009.09.085>.
- Vrij, A., Fisher, R., Mann, S., & Leal, S. (2006). Detecting deception by manipulating cognitive load. *Trends in Cognitive Sciences*, 10(4), 141–142, <http://dx.doi.org/10.1016/j.tics.2006.02.003>.
- Wallis, J. D., & Miller, E. K. (2003). Neuronal activity in primate dorsolateral and orbital prefrontal cortex during performance of a reward preference task. *European Journal of Neuroscience*, 18(7), 2069–2081, <http://dx.doi.org/10.1046/j.1460-9568.2003.02922.x>.
- Xu, F., Bao, X., Fu, G., Talwar, V., & Lee, K. (2010). Lying and truth-telling in children: from concept to action. *Child Development*, 81(2), 581–596, <http://dx.doi.org/10.1111/j.1467-8624.2009.01417.x>.
- Ye, J. C., Tak, S., Jang, K. E., Jung, J., & Jang, J. (2009). NIRS-SPM: statistical parametric mapping for near-infrared spectroscopy. *NeuroImage*, 44(2), 428–447, <http://dx.doi.org/10.1016/j.neuroimage.2008.08.036>.